# Ultra-fast and compact all optical Galois Field adder based on the LPhC structure and phase shift keying

Asghar Askarian[1], Fariborz Parandin[2], Nila Bagheri[3], and Fernando J. Velez[3*]

[1]Department of Electrical Engineering, Arak Branch, Islamic Azad University, Arak, Iran
[2]Department of Electrical Engineering, Kermanshah Branch, Islamic Azad University, Kermanshah, Iran
[3]Instituto de Telecomunicações and Universidade da Beira Interior, DEM – Faculdade de Engenharia, 6201-001 Covilhã, Portugal; e-mail: a.askarian92@iau-arak.ac.ir; fa.parandin@iau.ac.ir; nila.bagheri@ubi.pt; fjv@ubi.pt,
*Correspondence: fa.parandin@iau.ac.ir.

**Abstract**
In this study, we propose a novel all-optical Galois Field (AOGF) adder that utilizes logic all-optical XOR gates. The design is founded on the constructive and destructive interference phenomenon of optical beams and incorporates the phase shift keying (PSK) technique within a two-dimensional linear photonic crystal (2D-LPhC) structure. The suggested AOGF adder comprises eight input ports and four output ports. To obtain the electric field distribution in this structure, we employ the Finite Difference Time Domain (FDTD) procedure. The FDTD simulation results of the proposed AOGF adder demonstrate that the minimum and maximum values of the normalized power at ON and OFF states ($P_{1,min}$, $P_{0,max}$) for the output ports are 95% and 1.7%, respectively. Additionally, we obtain different functional parameters, including the ON-OFF contrast ratio, rise time, fall time, and total footprint, which are measured at 17.47 dB, 0.1 ps, 0.05 ps, and 147 μm$^2$, respectively.

**Keywords:** Photonic crystals, Optical Galois Field adder, Phase shift keying, Optical waveguide.

## 1. Introduction

Photonic crystals (PhCs) are artificial structures with periodic refractive index in a length comparable to the wavelength of the optical waves, which are fabricated in one-dimensional (1D), two-dimensional (2D) and three-dimensional (3D) forms [1-6]. The PhC structures can create photonic band gaps (PBGs) that prohibit the propagation of optical waves at certain wavelength ranges [7-12]. Two-dimensional Photonic crystal (2D-PhCs) structures have many advantages such as relatively easy design and fabrication, having a complete band gap, not depending on the angle of the incoming light, the ability to guide light inside optical waveguides and convenient integration compared to the other photonic devices [13-30]. Using PBG, various optical devices have been designed based on 2D-PhC, which greatly promotes the progress of optical integration [31-45]. PhCs have given rise to intriguing optical devices, and among them, all optical Galois Field (AOGF) adder is particularly noteworthy. This adder plays a crucial role in the design of all-optical digital systems used in communication coding and cryptography. AOGF adders are fundamental logic devices required for the development of these optical systems in the fields of communication coding and cryptography.

Recently, three research papers have proposed different approaches for designing AOGF adders using 2D-PhCs [46-48]. In this matter, Andalib [46] introduced the initial work on the implementation of an AOGF adder using optical waveguides based on a 2D linear photonic crystal (LPhC) structure. The logic structure was implemented based on the principle of beam interference, resulting in a delay time of approximately 1.5 ps and a footprint of 534 $\mu m^2$, respectively. In a separate study, Kharadmehr et al. [47] introduced the second AOGF adder utilizing nonlinear materials. The delay time and footprint of the structure were approximately 12 ps and 625 $\mu m^2$, respectively. Finally, Jalali et al. [48], in a third work, used four nonlinear resonant cavities for designing another AOGF adder. It had got the maximum ON-OFF contrast ratio of 16.02 dB.

Light signals are employed in optical fiber communication systems to transmit information across extensive distances. Optical fibers possess the capability to transmit signals swiftly and over long distances while experiencing minimal signal degradation. Consequently, they are exceptionally well-suited for high-bandwidth applications like internet communication, video streaming, and data center interconnects.

However, optical signals may experience several distortions as they travel through the fiber. These distortions can result from factors like as attenuation, dispersion, and noise. Attenuation corresponds to the loss of signal strength during propagation through the fiber, whereas dispersion leads to the signal spreading due to varying propagation speeds of different wavelengths of light. Noise can originate from various sources, including spontaneous emission, Raman scattering, and amplified spontaneous emission.

To ensure reliable communication over optical fibers, various signal processing techniques can be used to counteract these distortions and enhance the signal quality at the receiver end. For example, equalization techniques can be used to compensate for dispersion and reduce intermember interference, while forward error correction techniques can be used to detect and correct errors introduced by noise [49].

The Ultra-fast and compact all optical Galois Field adder based on LPhC structure and phase shift keying (PSK) technique is a specific technique for performing arithmetic operations in optical communication systems. Galois Field arithmetic is commonly used in error-correcting codes, which are essential for reliable communication over noisy channels. The LPhC structure and phase shift keying technique are used to implement Galois Field addition in an all-optical manner, which can be faster and more efficient than traditional electronic methods.

The LPhC structure is a type of photonic crystal structure that can be used to manipulate the properties of light. It consists of a periodic structure of high and low refractive index regions that can create band gaps in the optical spectrum. The phase shift keying technique is a modulation technique that can be used to encode information in the phase of an optical signal. By combining these techniques, it is possible to perform Galois Field addition in an all-optical manner.

The specific design and implementation details of an AOGF adder based on LPhC structure and (PSK) technique would depend on the specific requirements of the communication system and the desired performance characteristics. However, in general, it would involve designing and fabricating the necessary optical components, such as the LPhC structure and the phase shift keying modulator and developing appropriate signal processing algorithms to ensure proper

operation and compensate for any signal distortions introduced by the optical components or the transmission medium [50-52].

This paper presents the simulation of an AOGF adder using the 2D-LPhC structure, employing the plane wave expansion (PWE) and Finite Difference Time Domain (FDTD) methods, and modifying its different functional parameters. The proposed AOGF adder's functionality relies on the constructive and destructive interference principle of optical beams, in addition to the phase shift keying (PSK) technique [53, 54].

The upcoming parts of this paper will be presented in the following manner: Part 2 presents an overview of the structural design for the proposed AOGF adder, which integrates the LPhC structure and employs phase shift keying. Part 3 presents the simulation results obtained through the implementation of the FDTD procedure. Ultimately, Part 4 provides the concluding remarks.

**Structural design of the proposed AOGF adder**

A typical Galois Field (GF) adder can be constructed by combining four logic XOR gates, as shown in Figure 1, where there are eight input ports (labeled as A3, A2, A1 and A0 and B3, B2, B1 and B0) for two 4-bit Galois field codes and four output ports (labeled as F3, F2, F1 and F0) for the resulted output code [46].

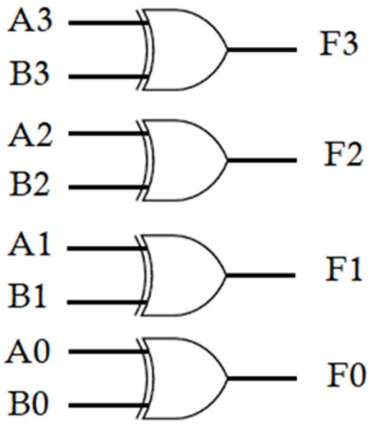


Figure1: The logic circuit of a typical GF adder.

The structure diagram of the suggested AOGF adder utilizing a 2D-LPhC is depicted in Figure 2, composed of four all optical logic XOR gates with square lattice. The lattice constant $a$ is set to be 550 nm, and the photonic crystals structure have a lateral size of $38a \times 13a$. The radius of the dielectric rods are composed of Silicon (Si) is 110 nm ($r = 0.2a = 110\ nm$), with refractive index $n_{Si}$ of 3.46. The Si rods are surrounded in the air ($n_{air} = 1$) background. The TM band gap of the proposed AOGF adder, as shown in Figure 3, is in the range of 0.282–0.417 ($a/\lambda$), where $\lambda$ denotes the optical wavelength in free space (the wavelength range is 1319–1950 nm). Table 1 provides a summary of the design parameters for the proposed AOGF adder.

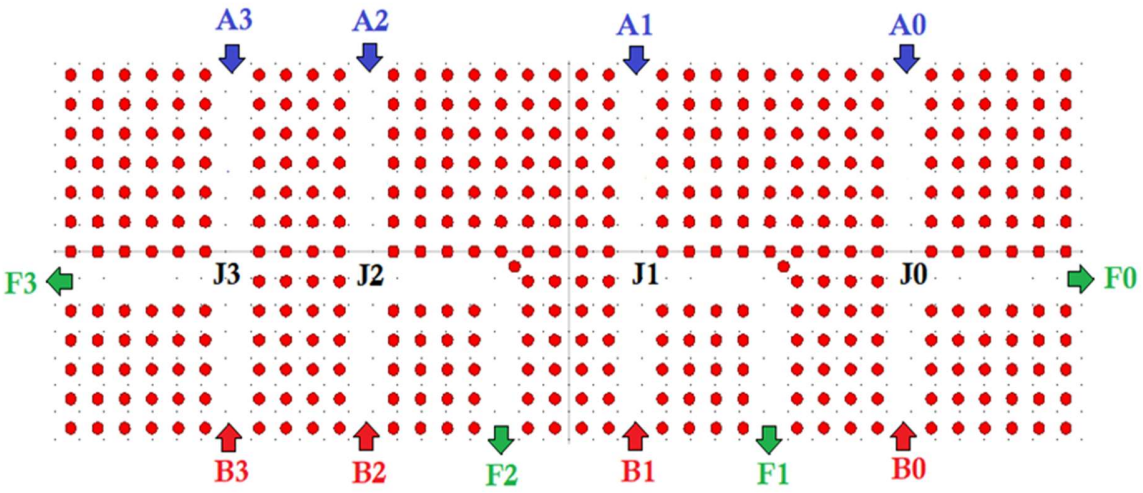


Figure 2. The final structure of the AOGF adder.

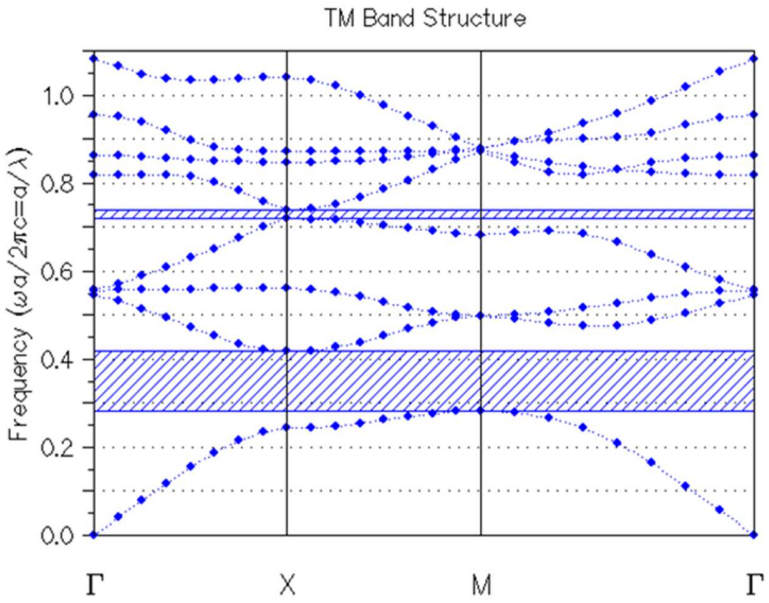


Figure 3. The TM band structure of the proposed AOGF adder based on LPhC structure and phase shift keying with the aforementioned values.

Table 1. presents the parameters of the proposed AOGF adder, which is based on the LPhC structure and incorporates PSK.

| Parameter | Value | Unit |
|---|---|---|
| Size of the lattice | 38×13 | - |
| Lattice constant (a) | 550 | nm |
| Index of Refraction for linear rods ( $n_{Si}$) | 3.46 | - |
| Refractive index of the background ($n_{air}$) | 1 | - |
| Fundamental rods' radius ($r$) | 110 | nm |
| Fundamental structure's total footprint | 147 | $\mu m^2$ |

## 2. Results and discussion

Following the design of the LPhC structure for the proposed AOGF adder, this section focuses on simulating and analyzing its performance. Four examples are considered, and the analysis is carried out using the 2D-FDTD procedure, which offers reduced calculation time compared to 3D simulations. The 2D-FDTD method is based on solving the Maxwell's equations ($\nabla \times \mathrm{H} = \frac{\partial \mathrm{D}}{\partial \mathrm{t}}$ and $\nabla \times \mathrm{E} = -\frac{\partial \mathrm{B}}{\partial \mathrm{t}}$) by discretizing the fields in space and time domain. In this method, the electromagnetic waves move along the X-Z plane. Hence, the Maxwell's equations are written as follows [55, 56]:

$$H_x^{n+\frac{1}{2}}(i,k) = H_x^{n-\frac{1}{2}}(i,k) - \frac{\Delta t}{\mu_{ik}\Delta z}\left[E_y^n(i,k+1) - E_y^n(i,k)\right] \quad (1)$$

$$H_z^{n+\frac{1}{2}}(i,k) = H_z^{n-\frac{1}{2}}(i,k) + \frac{\Delta t}{\mu_{ik}\Delta x}\left[E_y^n(i+1,k) - E_y^n(i,k)\right] \quad (2)$$

$$E_y^{n+1}(i,k) = E_y^n(i,k) + \frac{\Delta t}{\varepsilon_{ik}\Delta x}\left[H_z^{n+\frac{1}{2}}(i+1,k) - H_z^{n+\frac{1}{2}}(i,k)\right] - \frac{\Delta t}{\varepsilon_{ik}\Delta z}\left[H_x^{n+\frac{1}{2}}(i,k+1) - H_x^{n+\frac{1}{2}}(i,k)\right] \quad (3)$$

In the context of this study, we use the notations $n$, B, D, $E_y$, $H_x$, $H_z$, and ε to denote the discrete time step, magnetic induction field, electric displacement field, electric field in the y direction, magnetic field strength in the x direction, magnetic field strength in the z direction, and electric permittivity, respectively. The accuracy of the simulation results greatly depends on the appropriate selection of a spatial grid size that can effectively capture even the smallest details within the simulation field.

The space grids $\Delta x$ and $\Delta z$ (the x and z directions' mesh sizes) must be selected $\Delta x = \Delta z \leq \lambda/10$. In addition, the time and space grid are selected to satisfy the following condition:

$$\Delta t \leq \frac{1}{c}\sqrt{\left(\frac{1}{\Delta x}\right)^2 + \left(\frac{1}{\Delta z}\right)^2} \quad (4)$$

In this context, $c$ denotes the speed of light in free space. For this purpose, we excite the input ports with eight optical pulses (with optical intensity of 0.001 W/$\mu m^2$ at optical wavelength of 1550 nm). For the PSK technique, we used phases of 180º and 0º for the logic input signals 0 and 1,

respectively. For example, if phase of optical waves of ports $A1$ is 180º ($Ph_{A1} = 180°$), its corresponding logic level is zero ($A1 = 0$), and if phase of optical waves of these ports is 0º ($Ph_{A1} = 0°$), its corresponding logic level is one ($A1 = 1$). As mentioned above, the proposed AOGF adder consists of four optical XOR gates. In the simulation process, if the initial phase of the optical signals in the input ports of each gate is same, based on wave interference phenomenon and the difference in length of optical waveguides, its output is "0", and if the initial phase is different, its output is "1".

**Example 1: ($\mathbf{A = 0011}$ and $\mathbf{B = 1001}$)**

In this example, because the phase of optical waves of ports A2 and B2 is 180º ($Ph_{A2} = Ph_{B2} = 180°$ or $A2 = B2 = 0$), these waves will have destructive interference at J2 and eliminate each other and these light beams do not reach port F2 ($F2 = 0$). Also, because the phase of optical waves of ports A0 and B0 is 0º ($Ph_{A0} = Ph_{B0} = 0° \; deg$ or $A0 = B0 = 1$), these waves will have destructive interference at J0 and eliminate each other and these light beams do not reach port F0 ($F0 = 0$).

Because the phase of optical waves of ports $A3$ and $B3$ are 180 and 0º ($Ph_{A3} = 180°$ and $Ph_{B3} = 0°$ or $A3 = 0$ and $B3 = 1$), respectively, these waves will have constructive interference at J3. and their amplitude will be added to each other. Consequently, the result of light waves reaches port F3 ($F3 = 1$). Also, because the phase of optical waves of ports $A1$ and $B1$ are 0º and 180º ($Ph_{A1} = 0°$ and $Ph_{B1} = 180°$ or $A1 = 1$ and $B1 = 0$), respectively, these waves will have constructive interference at J1, and their amplitude will be added to each other and the result of light waves reaches port F1 ($F1 = 1$). As a result, the produced code will be 1010 ($F = 1010$) at the output ports (Figure 4a). According to the code generated at the output ports, it can be concluded that the proposed structure is AOGF adder. The output response curve of the proposed optical AOGF adder for this example is shown in Figure 4b. Based on this diagram, the normalized optical power at the F3, F2, F1 and F0 ports are 98% , 0.4% , 98% and 0.6% , respectively.

**Example 2: ($\mathbf{A = 0110}$ and $\mathbf{B = 0101}$)**

In this example, because the phase of optical waves of ports A3 and B3 is 180º ($Ph_{A3} = Ph_{B3} = 180°$ or $A3 = B3 = 0$), these waves will experience destructive interference at J3, causing them to cancel each other out, and as a result, these light beams will not reach port F3 (F3=0). Also, because the phase of optical waves of ports A2 and B2 is 0º ($Ph_{A2} = Ph_{B2} = 0°$ or $A2 = B2 = 1$), these waves will have destructive interference at J2 and eliminate each other and these light beams do not reach port F2 ($F2 = 0$). Because the phase of optical waves of ports $A1$ and $B1$ are 0º and 180º ($Ph_{A1} = 0°$ and $Ph_{B1} = 180°$ or $A1 = 1$ and $B1 = 0$), respectively, these waves will interact positively at J1, and when their amplitudes are summed, they form light waves that travel to port F1 (F1=1).

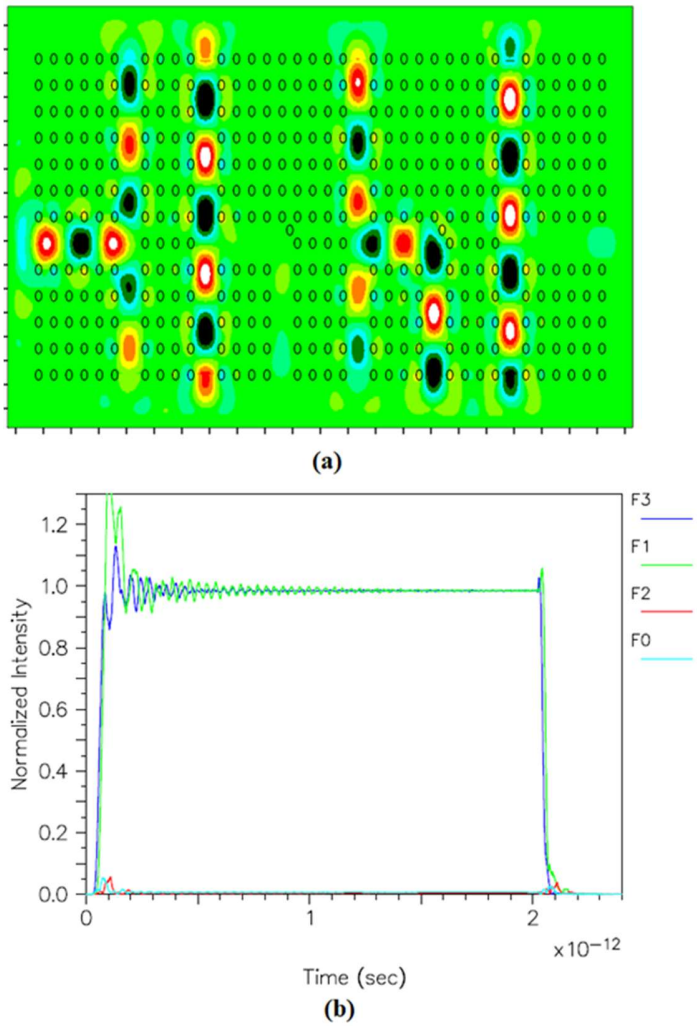


Figure 4. (a) The behavior of optical field propagation and (b) corresponding output time response curve of the proposed AOGF adder when A=0011 and B=1001.

Also, because the phase of optical waves at ports A0 and B0 is 180º and 0º ($Ph_{A0} = 180°$ and $Ph_{B0} = 0°$ or $A0 = 0$ and $B0 = 1$), respectively, these waves will undergo constructive interference at J0. Their amplitudes will add up, and as a result, the light waves will reach port F0 with a value of 1 (F0=1). Consequently, the produced code at the output ports will be 0011 (F=0011) as shown in Figure 5a.

Based on the output code observed at the ports, it can be deduced that the structure in question is indeed the AOGF adder. Figure 5b illustrates the response curve of the optical AOGF adder proposed in this instance. According to the diagram, the normalized optical power at ports F3, F2, F1, and F0 are determined to be 1%, 1.7%, 97%, and 99% respectively.

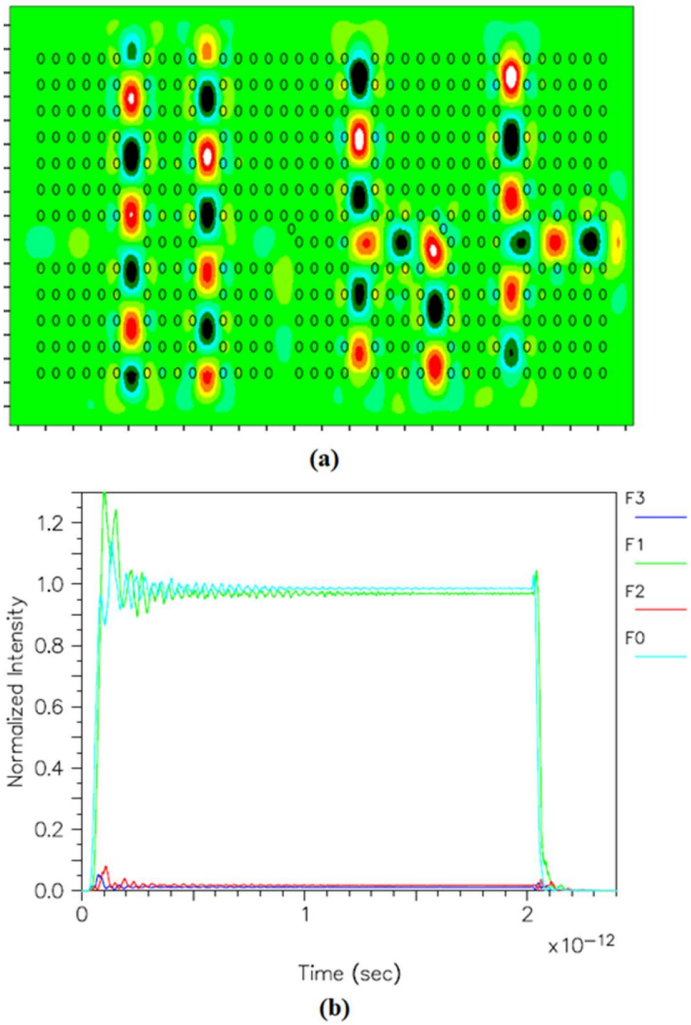


Figure 5. (a) illustrates (a) the optical field propagation behavior and (b) the corresponding output time response curve of the proposed AOGF adder when A=0110 and B=0101.

**Example 3: (A = 1100 and B = 1010)**

In this example, because the phase of optical waves of ports A3 and B3 is 0º ($Ph_{A3} = Ph_{B3} = 0°$ or A3 = B3 = 1), these waves will have destructive interference at J3 and eliminate each other and these light beams do not reach port F3 (F3 = 0). Also, because the phase of optical waves of ports A2 and B2 is 180 deg ($Ph_{A0} = Ph_{B0} = 180°$ or A0 = B0 = 0), The destructive interference of these waves at J0 causes them to cancel each other out, preventing them from traveling to port F0 (F0=0). Because the phase of optical waves of ports $A2$ and $B2$ are 0° and 180° ($Ph_{A2} = 0°$ and $Ph_{B2} = 180°$ or $A2 = 1$ and $B2 = 0$), respectively, these waves will have constructive interference at J2 and their amplitude will be added to each other and the result of light waves reaches port F2 (F2 = 1). Also, because the phase of optical waves of ports $A1$ and $B1$ are 180º and 0º ($Ph_{A1} = 180º$ and $Ph_{B1} = 0º$or $A1$ =0 and $B1$ =1), respectively, these waves will have constructive interference at J1 and their amplitude will be added to each other and the result of

light waves reaches port F1(F1=1). As a result, the produced code will be 0110 (F=0110) at the output ports, as shown in (Figure 6a). According to the code generated at the output ports, it can be concluded that the proposed structure is AOGF adder. The output response curve of the proposed optical AOGF adder for this example is shown in Figure 6b. Band based on this diagram, the normalized optical power at the F3, F2, F1 and F0 ports are 0.2%, 95%, 100% and 0.4%, respectively.

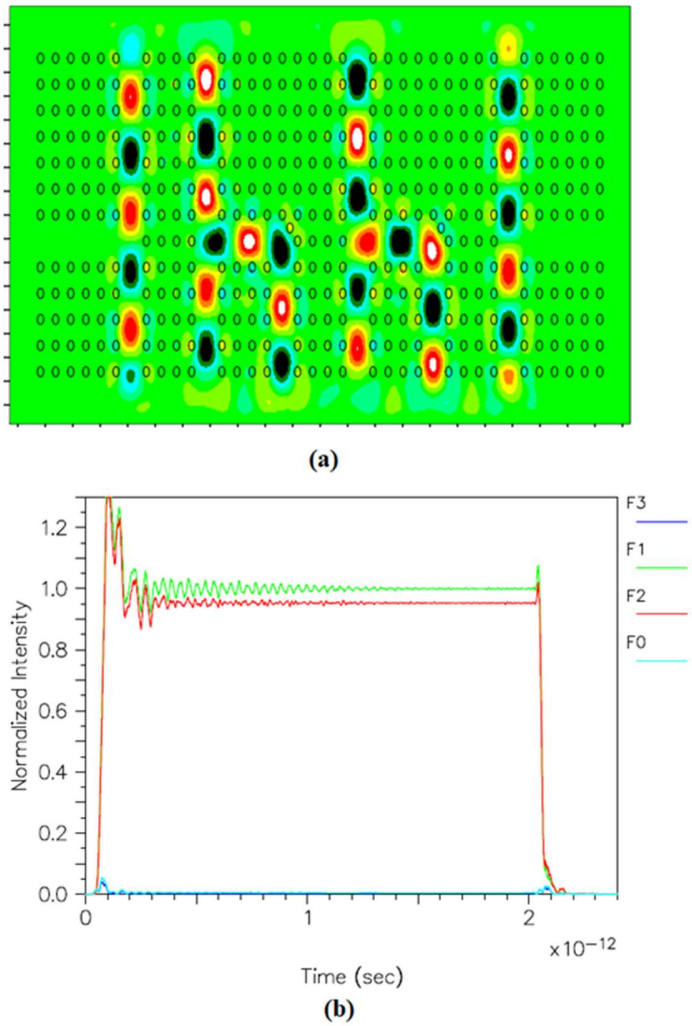


Figure 6. (a) The optical field propagation behavior and (b) corresponding output time response curve of the proposed AOGF adder when A=1100 and B=1010.

**Example 4: (A = 0110 and B = 1011)**

In this example, because the phase of optical waves of ports A1 and B1 is 0° ($Ph_{A1} = Ph_{B1} = 0°$ or A1 = B1 = 1), these light beams do not reach port F1 (F1=0) because at J1, these waves will experience destructive interference and cancel each other out. Because the phase of optical waves of ports $A3$ and $B3$ are 180 and 0º ($Ph_{A3} = 180°$ and $Ph_{B3} = 0°$ or $A3 = 0$ and $B3 = 1$), respectively, These waves will experience constructive interference at J3, and their amplitudes will be added together, resulting in the light waves reaching port F3 with a value of 1 (F3=1).

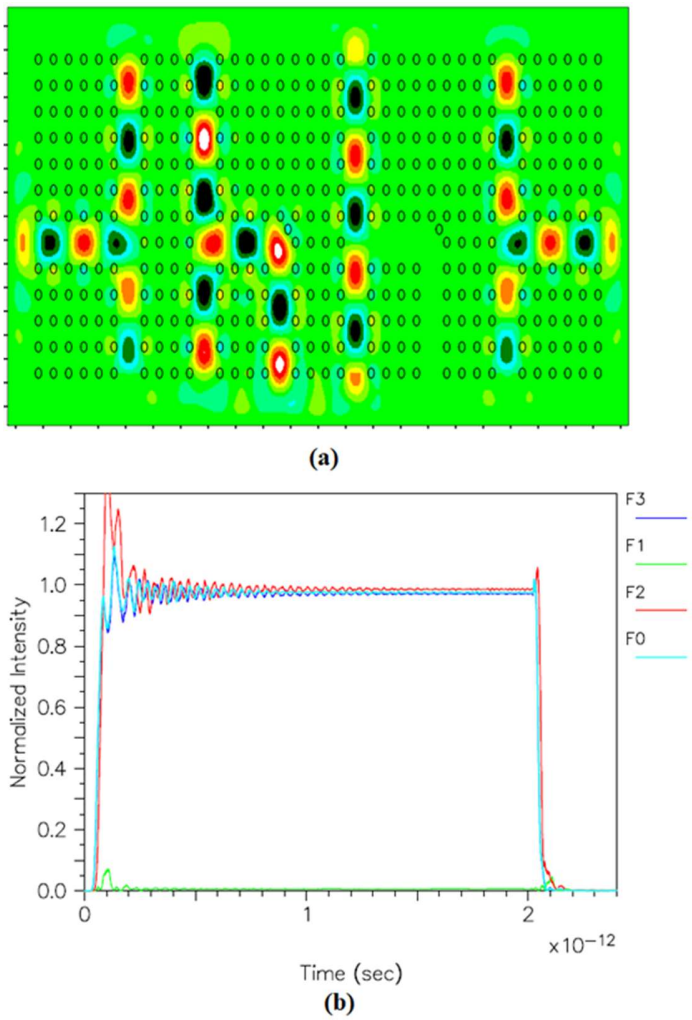


Figure 7. (a) The optical field propagation behavior and (b) corresponding output time response curve of the proposed AOGF adder when A=0110 and B=1011.

Also, because the phase of optical waves of ports $A2$ and $B2$ are 0º and 180º ($Ph_{A2} = 0°$ and $Ph_{B2} = 180°$ or $A2 = 1$ and $B2 = 0$), respectively, these waves will have constructive interference at J1 and their amplitude will be added to each other and the result of light waves reaches port F1 ($F2 = 1$). As the same way, because the phase of optical waves of ports $A0$ and $B0$ are 180º and 0º ($Ph_{A0} = 180°$ and $Ph_{B0} = 0°$ or $A0 = 0$ and $B0 = 1$), respectively, these waves will have constructive interference at J0 and their amplitude will be added to each other and the result of light waves reaches port F0 ($F0 = 1$). As a result, the produced code will be 1101 ($F = 1101$) at the output ports, as shown in Figure 7a. Based on the generated code observed at the output ports, it can be concluded that the proposed structure indeed corresponds to an AOGF adder. The response observed at the output curve of the proposed optical AOGF adder for this example is shown in Figure 7b and based on this diagram, the normalized optical power at the F3, F2, F1 and F0 ports are 97% , 98% , 0.6% and 97% , respectively.

The results obtained from the proposed AOGF adder including the normalized intensity and output codes have been summarized in Table 2. The output ports display a variety of normalized power

values in both the ON and OFF modes based on the information in Table 2's data. In particular, it is found that ($P_{1,min}$, $P_{0,max}$) have minimum and maximum normalized powers of 95% and 1.7%, respectively.
The rise, fall and delay times, bit rate and total footprint of the suggested AOGF adder are about 0.1ps, 0.05 ps, 0.2 ps, 5 Tbit/s and 147 $\mu m^2$, respectively.
A concise comparison of the attributes of the proposed AOGF adder with the designs documented in the literature is presented in Table 3. As shown in Table 3, the designed AOGF adder exhibits superior performance in terms of time delay, cross-section, and contrast ratio compared to all previously reported structures [36-38]. This demonstrates the efficient modification of its various functional parameters. As shown in Table 3, the size of the structure is 147 μm, which is smaller compared to other structures. The delay time is also obtained as 0.2 ps, which is significantly lower compared to the compared structures. Additionally, the proposed structure has a contrast ratio of 17.47 dB, which has somehow slightly increased.

Table 2. The obtained results of the proposed AOGF adder

| Input ports | | Normalized power at output ports (%) | | | | Output code |
|---|---|---|---|---|---|---|
| A | B | F3 | F2 | F1 | F0 | F |
| 0011 | 1001 | 98 | 0.4 | 98 | 0.6 | 1010 |
| 0110 | 0101 | 1 | 1.7 | 97 | 99 | 0011 |
| 1100 | 1010 | 0.2 | 95 | 100 | 0.4 | 0110 |
| 0110 | 1011 | 97 | 98 | 0.6 | 97 | 1101 |

Table 3. provides a brief overview of the characteristics of the AOGF adder in comparison to the currently available designs.

| Work | Mechanism | Delay time (ps) | Footprint ( $\mu m^2$) | Contrast ratio (dB) |
|---|---|---|---|---|
| Andalib [46] | Beams interference | 1.5 | 354 | 16.53 |
| Kharadmehr et al [47] | Threshold switching | 2.5 | 1210 | 16.02 |
| Jalali et al [48] | Threshold switching | 12 | 625 | 8.75 |
| This work | Combining beams interference and phase shift keying | 0.2 | 147 | 17.47 |

## 3. Conclusion

In this research paper, we conducted a simulation and evaluation of a 2D-LPhC-based AOGF adder using 2D plane wave expansion and 2D-FDTD methods. Phase shift keying and constructive and destructive optical beam interference are two phenomena that are essential to the proposed AOGF adder's operation. The results indicate that the designed AOGF adder exhibits superior time delay, cross-section, and contrast ratio compared to all previously reported structures, confirming the effective modification of its various functional parameters. Additionally, the suggested AOGF adder demonstrates a rise time, fall time, and total footprint of approximately 0.1 ps, 0.05 ps, and 147 $\mu m^2$, respectively. This adder has the potential to be

used in optical fiber communication systems to perform arithmetic operations on optical signals optically, such as adding or subtracting signals from different channels or wavelengths. This could enable more efficient use of the available bandwidth by allowing multiple signals to be combined or separated in a single device.

The proposed adder is also compact and ultra-fast, which could make it suitable for use in high-speed optical communication applications. The use of a 2D photonic crystal waveguide structure allows for strong light confinement, which can improve the efficiency and speed of signal processing. The use of PSK modulation also enables the encoding and decoding of information onto the light signal, which is important for optical communication systems.

The suggested all-optical Galois Field adder in the paper is a promising advancement in the field of optical communication since it has the potential to increase the effectiveness and speed of data processing in optical fiber communication systems. To improve the adder's performance and make sure it can be used in optical communication systems, more study and development are required.

## References


[1] Z. Fu, F. Sun, J. Zhou and H. Tian, "Highly Sensitive 1 × 8 Parallel Multiplexing of Ultra-Compact Integrated 1D Photonic Crystal Sensor Array Based on Silicon-on-Insulator Platform," in *IEEE Access*, vol. 8, pp. 65179-65186, 2020.

[2] A. Askarian, "Design and analysis of all optical half subtractor in 2D photonic crystal platform," *Optik* 228, 166126 (2021).

[3] E. Veisi, M. Seifouri and S. Olyaee, "A novel design of all-optical high speed and ultra-compact photonic crystal AND logic gate based on the Kerr effect," *Appl. Phys*. B 127, 70 (2021).

[4] N. A. Mohammed, O. E. Khedr, E. -S. M. El-Rabaie and A. A. M. Khalaf, "Literature Review: On-Chip Photonic Crystals and Photonic Crystal Fiber for Biosensing and Some Novel Trends," in *IEEE Access,* vol. 10, pp. 47419-47436, 2022.

[5] S. Serajmohammadi, H. Alipour-Banaei, and F. Mehdizadeh, "A novel proposal for all optical 1-bit comparator using nonlinear PhCRRs," *Photon. Nanostruct. Fundam. Applic*. 34, 19–23 (2019).

[6] A. Askarian, G. Akbarizadeh and M. Fartash, "An all-optical half subtractor based on kerr effect and photonic crystals," *Optik* 207, 164424 (2020).

[7] F. Mehdizadeh, M. Soroosh, H. Alipour-Banaei, and e. Farshidi, "A Novel proposal for all optical analog-to-digital converter based on photonic crystal structures, " *IEEE Photonics* J., 9, 5931–5935 (2017).

[8] Y. Zhao et al., "Sensitive and Robust Millimeter-Wave/Terahertz Photonic Crystal Chip for Biosensing Applications," in *IEEE Access*, vol. 10, pp. 92237-92248, 2022.

[9] M. Hosseinzadeh Sani, and S. Khosroabadi, "A novel design and analysis of high-sensitivity biosensor based on nano-cavity for detection of blood component, diabetes, cancer and glucose concentration, " *IEEE Sens*. J., 20, 7161-7168 (2020).

[10] R. Rajasekar, G. Thavasi Raja and S. Robinson, "Numerical analysis of reconfgurable and multifunctional barium titanate platform based on photonic crystal ring resonator, " *IEEE Trans.*

*Nanotechnol.* 20, 282–291 (2021).

[11] A. Askarian, G. Akbarizadeh, and M. Fartash, "A novel proposal for all optical half-subtractor based on photonic crystals," *Opt. Quantum Electron*. 51, 264 (2019).

[12] F. Parandin, M.-R. Malmir, M. Naseri and A. Zahedi, "Reconfigurable all-optical NOT, XOR, and NOR logic gates based on two dimensional photonic crystals," *Superlattices Microstruct*. 113, 737–744 (2017).

[13] E. G. Anagha and R. K. Jeyachitra, "Investigations on All-Optical Binary to Gray and Gray to Binary Code Converters Using 2D Photonic Crystals, " *IEEE J. Quant. Elec* 57, 6400310–6400310 (2021).

[14] H. Alipour-Banaei, M.G. Rabati, P. Abdollahzadeh-Badelbou and F. Mehdizadeh, "Effect of self-collimated beams on the operation of photonic crystal decoders," *J. Electromagn. Waves Appl*. 30 (2016) 1440–1448.

[15] W. Liu, D. Yang, G. Shen, H. Tian, and Y. Ji, "Design of ultra compact all-optical XOR, XNOR, NAND and OR gates using photonic crystal multi-mode interference waveguides," *Opt. Laser Technol.* 50, 55–64 (2013).

[16] C. Tang, X. Dou, Y. Lin, H. Yin, B. Wu, and Q. Zhao, "Design of all-optical logic gates avoiding external phase shifters in a twodimensional photonic crystal based on multi-mode interference for BPSK signals," *Opt. Commun*. 316, 49–55 (2014).

[17] N.M. D'souza and V. Mathew, "Interference based square lattice photonic crystal logic gates working with different wavelengths," *Opt Laser Technol*. 80 (2016) 214–19.

[18] J. Bao, J. Xiao, L. Fan, X. Li, Y. Hai and T. Zhang, " Design of alloptical logic gates avoiding external phase shifters in a twodimensional photonic crystal based on multi-mode interferencefor BPSK signals. ," *Opt Commun*. 377 (2014) 148–55.

[19] M. M. Karkhanehchi, F. Parandin, and A. Zahedi, "Design of an all optical half-adder based on 2D photonic crystals," *Photon. Netw. Commun*. 33, 159–165 (2016).

[20] S. Serajmohammadi, H. Alipour-Banaei, and F. Mehdizadeh, "Proposal for realizing an all-optical half adder based on photonic crystals," *Appl. Opt*. 57, 1617–1621 (2018).

[21] F. Parandin, A. Sheykhian and N. Bagheri, A novel design for an ultracompact optical majority gate based on a ring resonator on photonic crystal substrate. *J Comput Electron*, 2023.

[22] B. Mohammadi, M. Soroosh, A. Kovsarian, et al, "Improving the transmission efficiency in eight-channel all optical demultiplexers," *Photon Netw Commun* 38, 115–120, 2019.

[23] M.J. Maleki, M. Soroosh and A. Mir, "Ultra-fast all-optical 2-to-4 decoder based on a photonic crystal structure," *Appl. Opt*. 59, 5422-5428, 2020.

[24] M.J. Maleki, A. Mir and M. Soroosh, "Designing an ultra-fast all-optical full-adder based on nonlinear photonic crystal cavities", Opt Quant Electron 52, 196, 2020.

[25] F. Parandin, "Ultra-compact and low delay time all optical half adder based on photonic crystals," *Opt Quant Electron* 55, 398, 2023.

[26] Z. Seraj, M. Soroosh, N and Alaei-Sheini, "Ultra-compact ultra-fast 1-bit comparator based on a two-dimensional nonlinear photonic crystal structure," Appl. Opt. 59, 811-816, 2020.

[27] F. Parandin and N. Bagheri, "Design of a 2 × 1 multiplexer with a ring resonator based on 2D photonic

crystals," *Results in Optics*, 11, 100375, 2023.

[28] F. Parandin, F. Heidari, M. Aslinezhad, et al, "Design of 2D photonic crystal biosensor to detect blood components," *Opt Quant Electron* 54, 618 (2022).

[29] H. Saghaei, "Design and Simulation of an Ultra-Fast All-Optical Single-Bit Comparator Based on Photonic Crystal Ring Resonators," *JOURNAL OF APPLIED ELECTROMAGNETIC*, vol. 9, no. 2 (23) , pp. 99–106, 2022

[30] S. Naghizade, H. Saghaei, "Tunable electro-optic analog-to-digital converter using graphene nanoshells in photonic crystal ring resonators," *J. Opt*. Soc. Am. B 38, 2127-2134 (2021)

[31] M. Seifouri, S. Olyaee, M. Sardari, "Ultra-fast and compact all-optical half adder using 2D photonic crystals," *IET Optoelectron*. 13, 139–143 (2019).

[32] Y.-C. Jiang, S.-B. Liu, H.-F. Zhang, and X.-K. Kong, "Realization of all optical half-adder based on self-collimated beams by two-dimensional photonic crystals," *Opt. Commun*. 348, 90–94 (2015).

[33] A. Askarian, G. Akbarizadeh and M. Fartash, "All-optical half-subtractor based on photonic crystals," *Appl. Opt*. 58, 5931–5935 (2019).

[34] A. Askarian, "All optical half subtractor based on threshold switching and beams interference mechanisms," *J. Opt*. Commun. (2020).

[35] Y.-C. Jiang, S.-B. Liu, H.-F. Zhang, and X.-K. Kong, "Design of ultra-compact all optical half subtracter based on self-collimation in the two-dimensional photonic crystals," *Opt. Commun*. 356, 325–329 (2015).

[36] F. Parandin, M.-R. Malmir, and M. Naseri, "All-optical half-subtractor with low-time delay based on two-dimensional photonic crystals," *Superlattices Microstruct*. 109, 437–441 (2017).

[37] N. Namdari and R. Talebzadeh, "Simple and compact optical half-subtractor based on photonic crystal resonant cavities in silicon rods," *Appl. Opt*. 59, 165–170 (2020).

[38] A. Askarian, "Compact and ultra-fast all optical 1-bit comparator based on wave interference and threshold switching methods," *J. Opt*. Commun. (2021).

[39] Askarian. A, "Performance analysis of all optical 2 × 1 multiplexer in 2D photonic crystal structure," *J. Opt*. Commun. (2021).

[40] Askarian, A, " Design and implementation of all optical OR and NOR gates based on PhC structure and nonlinear Kerr effect," *J. Opt.* Commun. (2022).

[41] H. Jile, "Realization of an all-optical comparator using beam interference inside photonic crystal waveguides," *Appl. Opt.* 59, 3714–3719 (2020).

[42] H. Alipour-Banaei, M.G. Rabati, P. Abdollahzadeh-Badelbou, F. Mehdizadeh, "Application of self-collimated beams to realization of all optical photonic crystal encoder," Phys. E Low-Dimensional Syst. Nanostructures. 75 (2016) 77–85.

[43] Askarian, A., Parandin. F, "Numerical analysis of all optical 1‑bit comparator based on PhC structure for optical integrated circuits," *Opt Quant Electron* 55, 419 (2023).

[44] Askarian. A, Parandin. F, "A novel proposal for all optical 1bit comparator based on 2D linear photonic crystal," *J. Comput*. Electron. (2022).

[45] Askarian, A., Akbarizadeh, G., Fartash. M, "An all-optical half subtractor based on kerr effect and

photonic crystals," *Optik* 207, 164424 (2020).

[46] A. Andalib, "A novel proposal for all-optical Galois field adder based on photonic crystals, Photonic Netw," Commun. 35, 392–396 (2018).

[47] A. Kharadmehr, A. Andalib, "A novel proposal for an all-optical Galois field adder using nonlinear PhCRRs," *J. Comput*. Electron. 17 (2018) 1176–1180.

[48] P. Jalali, A. Andalib, "Application of nonlinear PhC-based resonant cavities for realizing all optical Galois Field adder," *Optik*, 180 (2019) 498–504.

[49] A. Askarian, "All optical half subtractor based on linear photonic crystals and phase shift keying technique," *J. Opt*. Commun. (2021).

[50] A. Askarian, "Design and analysis of all optical $2 \times 4$ decoder based on kerr effect and beams interference procedure," *Opt Quant Electron* 53, 291 (2021).

[51] S. J. B. Yoo, "Photonic Integrated Circuits for Communications, Signal Processing, and Computing Applications," in *Integrated Photonics and Nanophotonics Research and Applications*, (Optica Publishing Group, 2008), paper IWC2.

[52] Y. Lin, C. Tang, H. Yin, Y. Hao and C. Wu, "Design and optimization of all-optical AND and NOR logic gates in a two-dimensional photonic crystal for binary-phase-shift-keyed signals," *2014 7th International Conference on Biomedical Engineering and Informatics*, Dalian, China, 2014, pp. 965-969, doi: 10.1109/BMEI.2014.7002912.

[53] S. Naznin, S. T. Karim, R. T. Tisa and M. A. Farhad, "Design and simulation of all optical logic gates based on 2D photonic crystal fiber," *2015 International Conference on Electrical Engineering and Information Communication Technology (ICEEICT)*, Savar, Bangladesh, 2015, pp. 1-5, doi: 10.1109/ICEEICT.2015.7307499.

[54] Y. Lin, C. Tang, H. Yin, Y. Hao and C. Wu, "Design and optimization of all-optical AND and NOR logic gates in a two-dimensional photonic crystal for binary-phase-shift-keyed signals," *2014 7th International Conference on Biomedical Engineering and Informatics*, Dalian, China, 2014, pp. 965-969, doi: 10.1109/BMEI.2014.7002912.

[55] Taflove. A, "Computational Electrodynamics: The Finite-difference Time-domain Method,"*Artech House*, 1995.

[56] Hocini A, Harhouz. A," Modeling and analysis of the temperature sensitivity in two-dimensional photonic crystal microcavity," *J. Nanophoton*. 10, 016007 (2016).